Design and Development of Nanosized DNA Assemblies in Polypod-like Structures as Efficient Vehicles for Immunostimulatory CpG Motifs to Immune Cells

Kohta Mohri,[†] Makiya Nishikawa,[†,*] Natsuki Takahashi,[†] Tomoki Shiomi,[†] Nao Matsuoka,[†] Kohei Ogawa,[†] Masayuki Endo,[‡] Kumi Hidaka,[§] Hiroshi Sugiyama,[‡,§] Yuki Takahashi,[†] and Yoshinobu Takakura[†]

[†]Department of Biopharmaceutics and Drug Metabolism, Graduate School of Pharmaceutical Sciences, [‡]Institute for Integrated Cell-Material Sciences (iCeMS), and [§]Department of Chemistry, Graduate School of Science, Kyoto University, Sakyo-ku, Kyoto 606-8501, Japan

ABSTRACT The immunostimulatory activity of phosphodiester DNA containing unmethylated cytosine-phosphate-guanine (CpG) dinucleotides, or CpG motifs, was significantly increased by the formation of Y-, X-, or dendrimer-like multibranched shape. These results suggest the possibility that the activity of CpG DNA is a function of the structural properties of branched DNA assemblies. To elucidate the relationship between them, we have designed and developed nanosized DNA assemblies in polypod-like structures (polypod-like structured DNA, or polypodna for short) using oligodeoxynucleotides (ODNs) containing CpG motifs and investigated their structural and immunological properties. Those assemblies consisting of three (tripodna) to eight (octapodna) ODNs were successfully obtained, but one consisting of 12 ODNs was not when 36-mer ODNs were annealed under physiological sodium chloride concentration. High-speed atomic force microscopy revealed that these assemblies were in polypod-like structures. The apparent size of the products was about 10 nm in diameter, and there was an increasing trend with an increase in ODN length or with the pod number. Circular dichroism spectral data showed that DNA in polypodna preparations were in the B-form. The melting temperature of polypodna decreased with increasing pod number. Each polypodna induced the secretion of tumor necrosis factor-α and interleukin-6 from macrophage-like RAW264.7 cells, with the greatest induction by those with hexa- and octapodna. Increasing the pod number increased the uptake by RAW264.7 cells but reduced the stability in serum. These results indicate that CpG DNA-containing polypodna preparations with six or more pods are a promising nanosized device with biodegradability and high immunostimulatory activity.

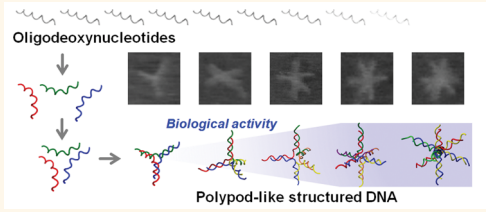

KEYWORDS: polypod-like structure · phosphodiester DNA · nanoassembly · CpG motif · macrophage

Recent advances on DNA nanotechnology have greatly widened the potential applications of DNA assemblies in a variety of fields. Some structured DNA assemblies have found their use in the sensitive detection of target compounds.[1,2] Furthermore, those with submicrometer diameters can be used as pharmaceutical agents or drug delivery devices[3] because this size range is suitable for controlling the cellular interaction as well as *in vivo* tissue distribution.

There are quite a few reports indicating that the innate immune stimulation is critical for the induction of adaptive immune responses.[4] The mammalian innate immune system can be activated through the ligation of Toll-like receptors (TLRs), including TLR9, which recognizes the DNA-containing CpG motif, an unmethylated cytosine-phosphate-guanine (CpG) dinucleotide flanked by some proper sequences.[5] Upon recognition by TLR9, CpG motif-containing DNA (CpG DNA), such as bacterial/viral DNA and synthetic oligodeoxynucleotides (ODNs), induce potent immune responses. Therefore, CpG DNA has been investigated as a therapeutic agent or an adjuvant for the treatment of a wide range of diseases, including cancer, viral infection, and allergic diseases.[6−9]

A variety of chemically stabilized DNA analogues have been developed to increase the potency of nucleic acid drugs,[10] but they are often associated with safety concerns.[11−14] Therefore, any approach to increasing the immunostimulatory activity of natural phosphodiester CpG DNA will greatly improve its potency without increasing the risk of adverse effects. Schmidt *et al.* reported that CpG DNA with a dumbbell-like covalently closed structure is effective in enhancing the inflammatory cytokine responses in human peripheral blood mononuclear cells.[15] Li *et al.* reported that DNA tetrahedra were effective in increasing the potency of phosphorothioate CpG DNA to induce cytokines from macrophages.[16] We previously reported that building up CpG

* Address correspondence to makiya@pharm.kyoto-u.ac.jp.

Received for review February 18, 2012 and accepted June 21, 2012.

Published online June 21, 2012
10.1021/nn300727j

DNA into a double-stranded, Y-shaped structure significantly increased the activity to produce cytokines upon addition to murine macrophage-like, TLR9-positive RAW264.7 cells.[17,18] Such DNA assemblies as Y-shaped DNA, or Y-DNA, can be used as building blocks for more complicated DNA products, such as dendrimer-like DNA and DNA hydrogels.[19,20] We also demonstrated that the dendrimer-like DNA consisting of CpG DNA-containing Y-DNAs was much more potent than the CpG DNA-containing Y-DNA in producing cytokines.[21,22]

These experimental results on the branched DNA assemblies containing CpG DNA provide clear evidence that the immunostimulatory activity of CpG DNA is a function of its tertiary structure. A variety of complicated DNA structures, including dendrimer-like DNA, DNA hydrogels, DNA origami, and DNA polyhedra, have been developed,[19,20,23,24] and their application as biological tools or pharmaceutical agents has been investigated.[25−27] Because some important properties of such DNA assemblies are a function of the structural properties, efficient and rational development of assembled DNA-based systems depends on a detailed understanding of the relationship between their structural and biological properties. Therefore, the optimization of the structure of DNA assemblies like Y-DNA will provide a new approach to increasing the potency of CpG DNA as adjuvants without any chemical modifications.

RESULTS AND DISCUSSION

There have been several reports on the structural properties of DNA assemblies, but there has been no systematic information on the relationship among the design and structural and biological properties of such branched DNA assemblies. Because some important properties of such DNA assemblies, including the immunostimulatory activity, are a function of the structural properties,[14,15] efficient and rational development of assembled DNA-based systems depends on a detailed understanding of their structural properties. Therefore, the present study examined first the structural properties of a series of nanosize ranged polypod-like structured DNA, or polypodna, preparations, and then the immunostimulatory activity of such assembled DNAs.

Three to twelve 36-mer ODNs (Table S1 in Supporting Information) were mixed to obtain tripodna$_{36}$ (three pods) to dodecapodna$_{36}$ (twelve pods) preparations, with the subscript number indicating the base length of the ODNs used. Each ODN was named as tripodna$_{36}$-1 and so on, with the base length as the subscript followed by the ODN number (#1 to #3 for tripodna, #1 to #4 for tetrapodna, and so on). Figure 1 shows the putative three-dimensional structures of some polypodna preparations. The formation of polypodna was determined by PAGE. Figure 2A shows the PAGE analysis of a variety of polypodna preparations.

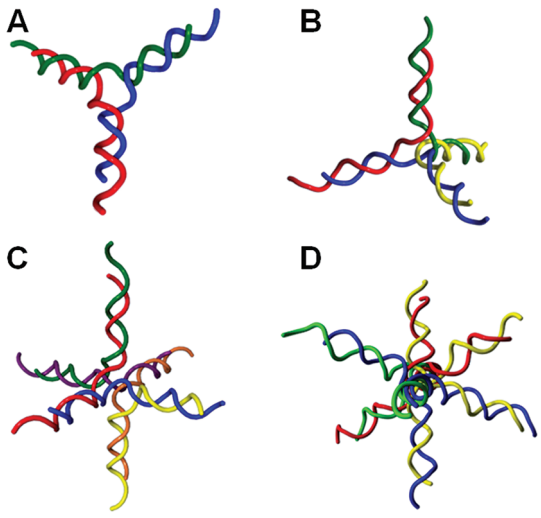

Figure 1. Schematic representation of putative structures of polypodna consisting of three, four, six, or eight ODNs: A, tripodna; B, tetrapodna; C, hexapodna; and D, octapodna.

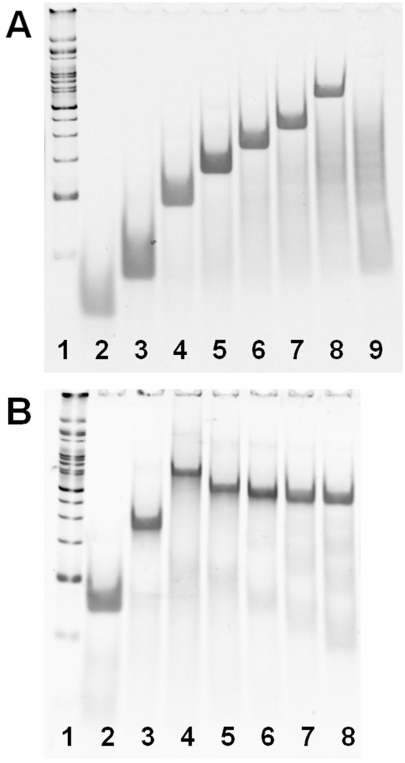

Figure 2. PAGE analysis of polypodna preparations with three to twelve pods. Each sample was run on a 6% polyacrylamide gel at 200 V for 20 min. A, lane 1, 100 bp DNA ladder; lane 2, ssDNA$_{36}$; lane 3, dsDNA$_{36}$; lane 4, tripodna$_{36}$; lane 5, tetrapodna$_{36}$; lane 6, pentapodna$_{36}$; lane 7, hexapodna$_{36}$; lane 8, octapodna$_{36}$; lane 9, dodecapodna$_{36}$. B, lane 1, 100 bp DNA ladder; lane 2, tripodna$_{30}$; lane 3, tripodna$_{60}$; lane 4, tripodna$_{90}$; lane 5, tripodna$_{80}$; lane 6, tetrapodna$_{60}$; lane 7, pentapodna$_{48}$; lane 8, hexapodna$_{40}$.

Tripodna$_{36}$, tetrapodna$_{36}$, pentapodna$_{36}$, hexapodna$_{36}$, and octapodna$_{36}$ had a major single band, indicating that the polypod-like structures were successfully formed with high efficiency by simple annealing of ODNs. On the other hand, no major bands were observed in the lane of

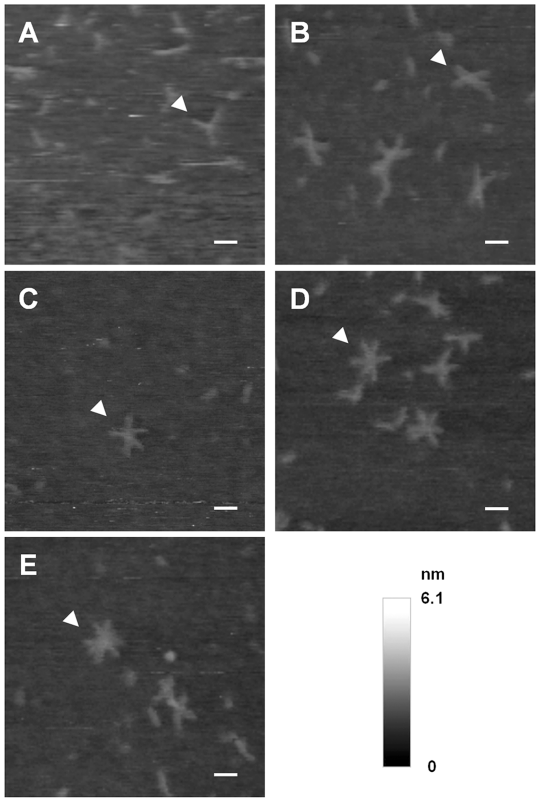

Figure 3. High-speed AFM images of polypodna preparations. AFM images of polypodna preparations were obtained in a buffer (20 mM Tris, 10 mM $MgCl_2$). A, tripodna$_{90}$; B, tetrapodna$_{90}$; C, pentapodna$_{90}$; D, hexapodna$_{90}$; and E, octapodna$_{90}$. Arrow heads indicate polypodna preparations captured in a structure extending the pods. The density scale is shown in the right bottom of the figure. White bars in the images indicate 20 nm. Image size, 225 nm × 225 nm.

dodecapodna$_{36}$ (Figure 2A, lane 9). The mobility of polypodna decreased with an increasing number of pods. Figure 2B shows the PAGE analysis of tripodna consisting of ODNs of 30, 60, or 90 nucleotides. The migration distance became shorter on increasing the ODN length in tripodna. Therefore, the migration distance of polypodna seems to be determined by the number of bases in polypodna preparations. To confirm this, a variety of polypodna consisting of 240 nucleotides were designed using ODNs with different lengths. The mobility of tripodna$_{80}$, tetrapodna$_{60}$, pentapodna$_{48}$, and hexapodna$_{40}$ was almost identical (Figure 2B), strongly suggesting that the migration distance depends largely on the number of nucleotides but not on the steric properties of the structures.

The formation of polypodna was visually confirmed by observation with high-speed atomic force microscopy (AFM). Because of the limitation of the resolution, a series of 90-mer ODNs (Table S1) were used for the preparation of tripodna$_{90}$, tetrapodna$_{90}$, pentapodna$_{90}$, hexapodna$_{90}$, and octapodna$_{90}$. The formation of these polypodna preparations consisting of 90-mer ODNs was

TABLE 1. T_m Value and Apparent Size of dsDNA and Polypodna Preparations

DNA	T_m[a] (°C)	size (nm)
dsDNA$_{36}$	66.5	ND
tripodna$_{36}$	54.6	6.2
tetrapodna$_{36}$	50.8	7.4[b]
pentapodna$_{36}$	47.9	7.7[b]
hexapodna$_{36}$	44.8	8.2[b]
octapodna$_{36}$	43.9	8.3[b]
tripodna$_{30}$	46.5	ND
tripodna$_{60}$	61.2	8.9[c]
tripodna$_{90}$	68.3	12.1
tripodna$_{80}$	64.9	10.7[e,f,g]
tetrapodna$_{60}$	59.8	9.1[d,g]
pentapodna$_{48}$	53.2	8.5[d,g]
hexapodna$_{40}$	48.5	6.5[d,e,f]

[a] The melting temperature (T_m) values were calculated from melting curves of DNA samples in a TE buffer solution (pH 8) containing 5 mM sodium chloride. The size was measured by DLS and expressed as the mean of three (tripodna$_{36}$, tetrapodna$_{36}$, pentapodna$_{36}$, hexapodna$_{36}$, tripodna$_{80}$, tetrapodna$_{60}$, pentapodna$_{48}$, hexapodna$_{40}$) or six (octapodna$_{36}$, tripodna$_{60}$, tripodna$_{90}$) determinations. [b] $P < 0.05$ from tripodna$_{36}$. [c] $P < 0.05$ from tripodna$_{90}$. [d] $P < 0.05$ from tripodna$_{80}$. [e] $P < 0.05$ from tetrapodna$_{60}$. [f] $P < 0.05$ from pentapodna$_{48}$. [g] $P < 0.05$ from hexapodna$_{40}$. In all cases, the SE values of the size were less than 5% of the mean. ND, not determined.

first checked by PAGE (data not shown). The AFM images clearly showed that all of the preparations were in polypod-like structures with exactly the same numbers of pods as the numbers of ODNs used (Figure 3). Namely, three, four, five, six, and eight pods expanded outward from the center of the structures for tri-, tetra-, penta-, hexa-, and octapodna$_{90}$, respectively. Previous studies reported the AFM images of branched structures of Y- or X-DNA.[28,29] The images of tripodna$_{90}$ and tetrapodna$_{90}$ of the present study were in good agreement with these previous ones. The AFM images of five or more branched DNA assemblies were obtained for the first time as far as we know, which clearly indicated that each polypodna preparation has a core and the same numbers of pods as the numbers of ODNs used. Because the DNA samples were adsorbed onto mica plates for imaging, the structure of polypodna should be distorted due to the adsorption to the flat surface. This could be a reason why there were several DNA assemblies with incomplete or distorted structures in the AFM images. Together, these results provide the experimental evidence that annealing three or more ODNs with the halves of each ODN being complementary to a half of other two ODNs results in the formation of nanosized polypod-like structured DNA assemblies.

The thermal stability of polypodna preparations obtained was evaluated by measuring the melting temperature (T_m). Table 1 summarizes the T_m values of double-stranded (ds) DNA$_{36}$ and a variety of polypodna preparations in TE buffer (pH 8) containing 5 mM sodium chloride. The T_m of dsDNA$_{36}$ was higher than those of other preparations using 36-mer ODNs.

The T_m was found to be a function of the pod number, and the larger the pod number the lower the T_m. Because the length of ODN was the same for all of these preparations, these results suggest that the double-strand formation or hybridization becomes less complete when the pod number increases. Then, the T_m values of tripodna preparations were found to be dependent on the ODN length, and one with the longest ODN (*i.e.*, tripodna$_{90}$) had the highest T_m. Under the conditions used in the present study, dodecapodna$_{36}$ was not obtained (Figure 2A). The reason for this would be because the thermal stability of dodecapodna was too low, and there should be a critical point between eight and twelve pods as far as polypodna formation is concerned. A previous study reported that DNA with twelve pods was formed using 48-mer ODNs,[30] suggesting that the critical pod number for polypodna formation is dependent on ODN length and on the salt type and concentration, pH, and other buffer variables. However, from a pharmaceutical point of view, nonphysiological conditions are not suitable, and very long ODNs are not proper in terms of cost and purity. Therefore, one conclusion that can be drawn from the present study is that polypodna preparations with eight or fewer pods are suitable for the use to increase the potency of CpG DNA.

The decrease in T_m can be due to the reduced efficiency of hybridization. The replacement of some bases in the central region with noncomplementary sequences reduced the T_m of both dsDNA and hexapodna (unpublished data). These experimental data suggest that all of the bases in polypodna preparations, even ones close to the center of the assemblies where ODNs should be forced to bend sharply, are involved in the structural and thermal stability. In other words, an increasing pod number will lead to structural impairment in the central part, followed by a reduced stacking of bases. This hypothesis is supported by previous studies based on crystal analysis, which showed that some bases in the central part of DNA assemblies like tetrapodna were not properly stacked.[31]

The apparent size of polypodna preparations was measured assuming that the shape of the DNA structures was noncircular (Table 1). All of the preparations were in the nanosize range and had a narrow distribution. The apparent size of tripodna preparations increased on increasing the ODN length from 36 to 90. Furthermore, the size of the polypodna containing 240 bases, such as tripodna$_{80}$, tetrapodna$_{60}$, pentapodna$_{48}$, and hexapodna$_{40}$, also depended on the ODN length. When the polypodna preparations consisting of 36-mer ODNs were compared, the size was slightly, but significantly, increased on increasing the pod number. These results could also be explained by the hypothesis that the reduced stacking of bases in polypodna preparations with many pods leads to some swelling of the structures.

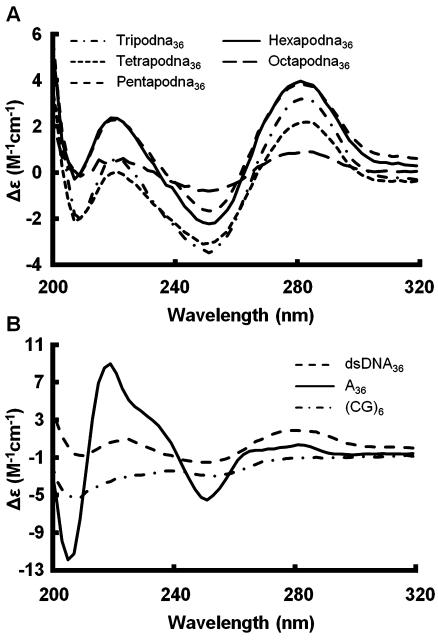

Figure 4. CD spectra of DNA preparations. CD spectra were recorded using a JASCO-820 type spectropolarimeter. To facilitate comparisons, the CD spectra were background subtracted and smoothed.

Figure 4 shows the circular dichroism (CD) spectra of several types of DNA preparations. dsDNA$_{36}$ had positive and negative peaks near 280 and 240 nm, respectively, which is typical of spectra of the B-form DNA.[32] Every polypodna showed a profile similar to that of dsDNA$_{36}$ (Figure 4A). Figure 4B shows the CD spectra of A$_{36}$ and (CG)$_6$, both of which are known to be in non-B-forms,[32,33] together with that of hexapodna$_{36}$. A$_{36}$ and (CG)$_6$, the latter being a Z-form DNA, exhibited profiles that were different from those of dsDNA$_{36}$, suggesting that polypodna possess the spectral characteristics of B-form DNA. The favored form of double-stranded DNA is B-DNA at a high humidity and low salt concentration similar to that found under physiological conditions. Thus, these results suggest that the double-stranded DNA parts are like those under normal conditions. Some DNA sequences like CGCGCG have been known to be in the Z-form, a left-handed helical structure.[33] It is an open question about the structural properties of DNA assemblies when DNA in the Z-form is used.

Figure 5 shows the tumor necrosis factor (TNF)-α and interleukin (IL)-6 concentrations in the culture media of RAW264.7 cells after addition of single-stranded (ss) DNA, dsDNA, or polypodna preparations containing CpG motifs. All CpG DNA samples induced the TNF-α release from RAW264.7 cells depending on the concentrations of DNA (Figure 5A). However, only small amounts of TNF-α were released when ssDNA or dsDNA was added to cells. In contrast, polypodna preparations induced the release of large amounts of TNF-α, even though the same amounts of DNA as ss- or

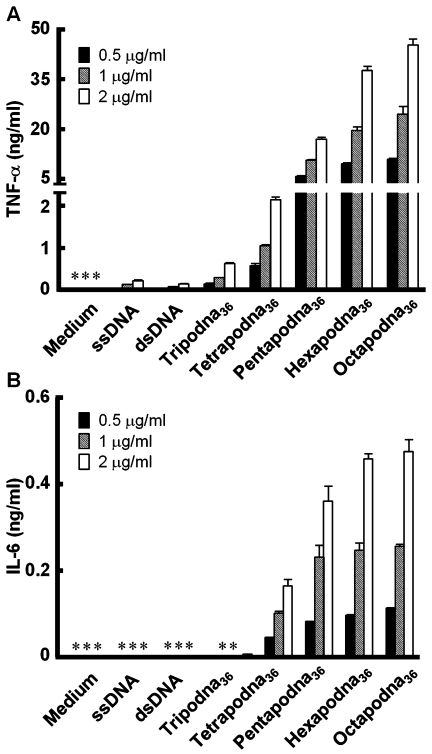

Figure 5. Cytokine release from RAW264.7 cells by DNA preparations. Each sample in Opti-MEM was added to cells at a final concentration of 0.5, 1, or 2 μg/mL, and the concentrations of TNF-α (A) and IL-6 (B) in culture media were measured at 8 h. Results are expressed as mean $\pm$ SD of three determinations. Data are representative of four (A) or two (B) independent experiments. *, Values were under the detection limit.

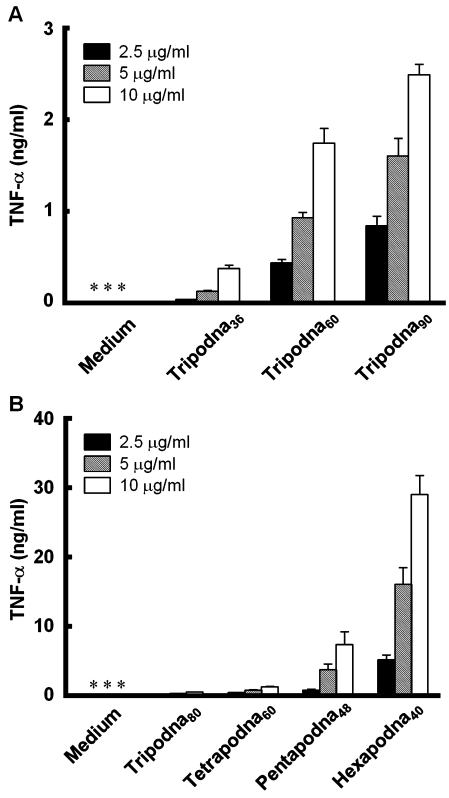

Figure 6. TNF-α release from RAW264.7 cells by polypodna preparations. Each sample in Opti-MEM was added to cells at a final concentration of 2.5, 5, or 10 μg/mL, and the concentrations of TNF-α in culture media were measured at 8 h. Results are expressed as mean $\pm$ SD of three determinations. Data are representative of four (A) or three (B) independent experiments. *, Values were under the detection limit.

dsDNA were added to cells. Furthermore, the pod number had a great impact on the amount of TNF-α release, and the amount was greatly increased with an increasing pod number. Similar results were obtained for the IL-6 release from RAW264.7 cells (Figure 5B). These results indicate that polypodna with many pods are suitable structures to increase the immunostimulatory activity of CpG DNA.

Polypodna preparations with more pods have more nucleotides in one unit than ones with fewer pods, so the large number of nucleotides in one unit could be a reason for the high potency of polypodna preparations with many pods, such as hexapodna and octapodna. Thus, the effect of the number of nucleotides in polypodna on cytokine release was investigated using tripodna preparations with different pod lengths: tripodna$_{30}$, tripodna$_{60}$, and tripodna$_{90}$. To minimize the differences in the sequence among the preparations, a sequence of 30 base pairs containing one potent CpG motif was repeatedly used to prepare tripodna$_{30}$, tripodna$_{60}$, and tripodna$_{90}$ (Table S1). Figure 6A shows the TNF-α concentrations in the culture media of RAW264.7 cells after addition of the tripodna preparations. The amounts of TNF-α released were increased with an increasing number of nucleotides in tripodna, even though the same amounts of DNA were added to the cells. To confirm the importance of pod number apart from the number of nucleotides, the immunostimulatory activity of polypodna preparations consisting of 240 nucleotides (*i.e.*, tripodna$_{80}$, tetrapodna$_{60}$, pentapodna$_{48}$, hexapodna$_{40}$) was compared. Figure 6B shows the TNF-α concentrations in the culture media of RAW264.7 cells after addition of these polypodna preparations. Among those examined, hexapodna$_{40}$ induced the greatest release of TNF-α, followed by pentapodna$_{48}$, tetrapodna$_{60}$, tripodna$_{80}$, in this order, even though hexapodna$_{40}$ was constructed with the shortest ODNs among those compared. These results indicate that increasing the pod number is effective in increasing the immunostimulatory activity of CpG DNA irrespective of the number of nucleotides in one unit.

Cellular uptake of CpG DNA is one of the factors determining the amount of cytokines released from cells. Thus, the cellular uptake of polypodna was investigated using Alexa Fluor 488-labeled DNA samples. Figure 7A shows the normalized MFI of RAW264.7 cells after addition of Alexa Fluor 488-labeled ssDNA$_{36}$, dsDNA$_{36}$, or polypodna$_{36}$ with three, four, five, six, or eight pods. In all cases examined, the normalized MFI values at 37 °C were higher than those at 4 °C (data not shown), suggesting that DNA was taken up by cells at

the higher temperature. At both concentrations examined, the normalized MFI values were the highest for octapodna$_{36}$, followed by hexa-, penta-, tetra-, tripodna$_{36}$, dsDNA$_{36}$, and ssDNA$_{36}$ in this order. The rank order in cellular uptake was exactly the same as that in the cytokine release (Figure 5). Then, the cellular uptake of polypodna preparations consisting of 240 nucleotides was also investigated by measuring the remaining amounts of these DNA preparations in culture media. The amount of DNA in culture media hardly decreased with time when incubated with cells at 4 °C or without cells at 37 °C (data not shown), so the disappearance of DNA from culture media was used to estimate cellular uptake of polypodna preparations. Hexapodna$_{40}$ and pentapodna$_{48}$ disappeared most quickly, followed by tetrapodna$_{60}$ and tripodna$_{80}$ in this order (Figure S1). These results strongly suggest that the efficient cellular uptake is one of the reasons why polypodna preparations with many pods are effective in inducing cytokine release.

To examine the mechanism of the cellular uptake of these DNA preparations, Alexa Fluor 488-labeled tripodna$_{36}$ was added to cells with or without unlabeled DNA preparations. Figure 7B shows the MFI values of RAW264.7 cells at 2 h after addition of Alexa Fluor 488-labeled tripodna$_{36}$. Addition of unlabeled tripodna$_{36}$ resulted in the reduction of the MFI values in a dose-dependent manner, suggesting that the uptake is a saturable process. The uptake of Alexa Fluor 488-labeled tripodna$_{36}$ was inhibited by the addition of dsDNA or any polypodna$_{36}$ preparation. Octapodna$_{36}$ showed the strongest potency to inhibit the uptake, followed by hexapodna$_{36}$, pentapodna$_{36}$, and so on, with ssDNA being the least. These results strongly suggest that these polypodna preparations are taken up by cells through the same mechanisms as ss- and dsDNA, and the affinity for the uptake is increased with increasing pod number. Qualitatively similar results were obtained when Alexa Fluor 488-labeled hexapodna$_{36}$ was used for the competitive studies (Figure S2). Figure 7C–F shows the images of RAW264.7 cells added with Alexa Fluor 488-labeled hexapodna$_{36}$. The fluorescence signals were detected within the cells as punctate forms, suggesting its uptake by endocytosis. Similar results were observed using other polypodna preparations (data not shown). It was reported that longer DNA are taken up by cells more efficiently than shorter ones.[34] These previous findings, as well as our present results of tripodna preparations with different sizes (Figure 6A), suggest that the internalization is accelerated by multiple interactions between DNA and cell surface, although the mechanism of the interaction and components involved in it have not been fully understood.[35,36] When polypodna are constructed using 36-mer ODNs, one unit of each polypodna contains 108, 144, 180, 216, and 288 nucleotides for tri-, tetra-, penta-, hexa-, and octapodna, respectively. Thus, the uptake of one unit of polypodna results in different amounts of DNA taken up by cells depending on the pod number.

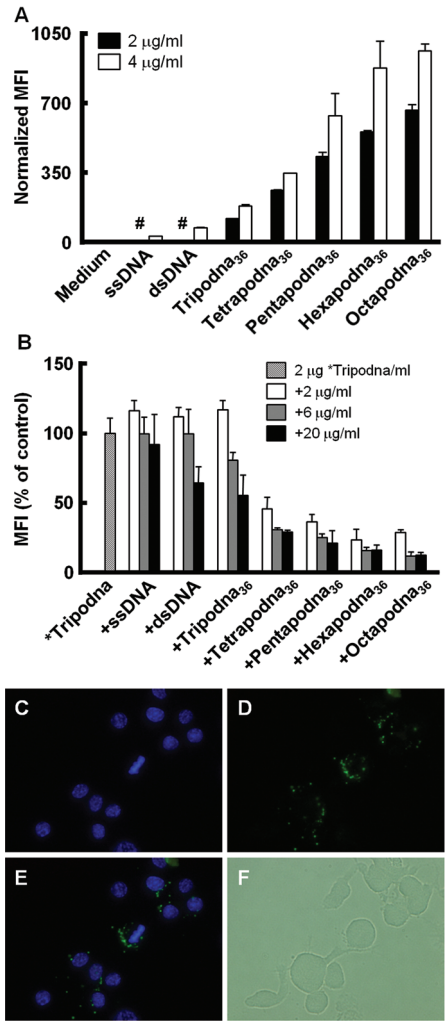

Figure 7. Uptake of DNA preparations in RAW264.7 cells. (A) Each Alexa Fluor 488-labeled DNA sample in Opti-MEM was added to cells at a final concentration of 2 or 4 μg/mL, and cells were incubated for 8 h at 37 °C. The amounts of DNA associated with cells were measured by flow cytometry, and the normalized MFI was calculated to compare the cellular uptake of these DNA preparations. Results are expressed as the mean ± SD of three determinations. Data are representative of three independent experiments. #, Values were not evaluated. (B) Alexa Fluor 488-labeled tripodna$_{36}$ in Opti-MEM was added to cells at a final concentration of 2 μg/mL with or without unlabeled DNA samples at a concentration of 2, 6, or 20 μg/mL, and cells were incubated for 2 h at 37 °C. Results are normalized to the MFI of the control group (*tripodna, without unlabeled DNA) and are expressed as the mean ± SD of three determinations. (C–F) Typical images of RAW264.7 cells after addition of Alexa Fluor 488-labeled hexapodna$_{36}$. Cells were counterstained with DAPI to visualize the nuclear DNA. (C) DAPI staining; (D) Alexa Fluor 488-labeled hexapodna$_{36}$; (E) merged image; and (F) bright field.

The stability of CpG DNA is another important parameter determining its potency. Our previous studies showed that Y-DNA is less stable than dsDNA.[17,18] Therefore, the effect of pod number of polypodna

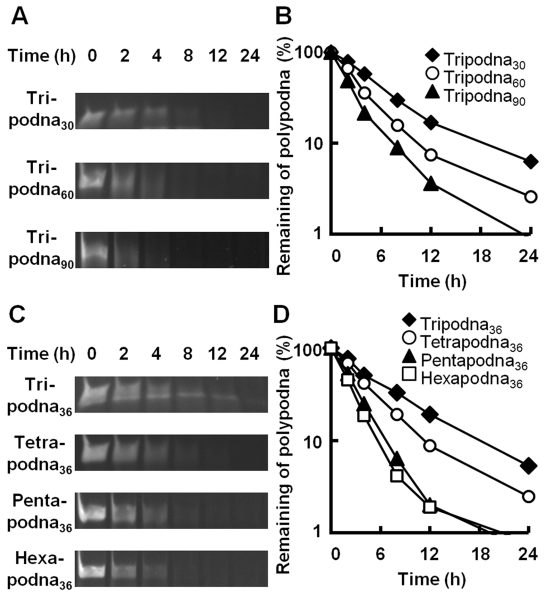

Figure 8. Degradation of polypodna preparations in mouse serum. (A,C) Polypodna preparations were incubated in 20% mouse serum at a concentration of 100 μg/mL at 37 °C, and the reaction was terminated at indicated periods of time by adding EDTA. The samples were run on 12% PAGE at 4 °C and stained with SYBR Gold. (B,D) Amounts of remaining polypodna were plotted against incubation time. These experiments were performed three times with similar results, and one representative gel is shown.

on the stability in mouse serum was investigated (Figure 8). All polypodna preparations were degraded with time. The longer the pod length of tripodna, the faster the degradation rate (Figure 8A,B). Then, the polypodna preparations consisting of 36-mer ODNs were compared (Figure 8C,D). Although polypodna preparations with many pods were more effective in inducing cytokine release, they were less stable in mouse serum (Figure 8). DNA is mainly degraded by exonucleases in biological fluids,[37] so that one with many ends, like hexa- and octapodna, will be quickly degraded than one with fewer ends. Therefore, increasing pod number can be a trade-off between efficient interaction with TLR9 and low enzymatic stability, but the results of the present study have shown that the pod number-dependent reduction in the stability would not have large impact on the immunostimulatory activity of polypodna.

The results of the present study together with a previous one[21] show that the pod number-dependent increase in the amounts of cytokine release is much greater than the increase in cellular uptake (Figures 5 and 7A), suggesting that other factors than the uptake is involved in the effective induction of cytokines with polypodna preparations with many pods. Double-strand formation greatly reduced the immunostimulatory activity of CpG DNA,[38] and this reduction has been explained by experimental evidence that TLR9 binds single-stranded CpG DNA.[39] Because the T_m of polypodna was a function of the pod number and decreased with increasing pod number (Table 1), CpG DNA in polypodna with many pods would more easily become single stranded. To confirm this speculation, we evaluated the dissociation of the assembled DNA in and outside of cells by measuring the T_m values of DNA samples under simulated extracellular (pH 7.4, a high sodium concentration) and endosomal (pH 5.5, a medium sodium concentration) conditions.[40] Irrespective of the samples, the T_m values under the simulated endosomal conditions were lower than those under the extracellular ones (Table S2). Under the low pH condition, the T_m of polypodna decreased with increasing pod number. Taken together, it can be concluded that the significant increase in the immunostimulatory activity of CpG DNA by building it up into hexa- or octapodna is due to an efficient uptake by TLR9-positive cells and a facilitated dissociation to single strands. The results of polypodna consisting of 240 nucleotides (Figure 6B) also indicated that increasing the pod number is more effective than increasing the ODN length for increasing the amounts of cytokines released from TLR9-positive cells.

It is important whether these polypodna preparations are more effective than ss- or dsDNA in inducing cytokine production not only in cultured cells but also *in vivo*. In a different set of experiments, we prepared six ODNs of 40 nucleotides and developed a hexapodna preparation containing CpG motifs. When injected into the dorsal skin of mice, this hexapodna preparation induced significantly higher mRNA expression of IL-6 at the injection site than its component, that is, single-stranded CpG DNA (Nishikawa *et al.*, manuscript in preparation). Together with the findings of the present study of the pod number-dependent increase in the immunostimulatory activity of CpG DNA, these results support the notion that polypodna preparations with many pods are effective in inducing cytokine production also *in vivo*.

A variety of other nanosized systems, including liposomes and gold nanoparticles, have been used for delivering CpG DNA to stimulate the innate immune cells.[41,42] Recent examples include tertiary-structured DNA origami and tetrahedral DNA, which increased the immunostimulatory activity of CpG DNA.[16,43] It is interesting to compare the present results with those reported in the literature. However, it is an open question whether these other systems are effective for the delivery of natural phosphodiester CpG DNA, not phosphorothioate-stabilized ones.

CONCLUSION

We have demonstrated that polypodna preparations with three to eight pods can be constructed under physiological conditions, and their polypod-like structures were clearly shown in AFM images. Increasing pod number is directly linked with reduced thermal stability, efficient cellular uptake, and large amount of

cytokine production from TLR9-positive cells. These findings provide useful information on the use of these nanosized DNA assemblies for safe and efficient adjuvants or immunostimulatory agents.

MATERIALS AND METHODS

Chemicals. RPMI1640 medium was obtained from Nissui Pharmaceutical Co., Ltd. (Tokyo, Japan). Fetal bovine serum (FBS) was obtained from Equitech-Bio, Inc. (Kerrville, TX, USA). Opti-modified Eagle's medium (Opti-MEM) was purchased from Invitrogen (Carlsbad, CA, USA). The 100 bp ladder was purchased from Watson (Tokyo, Japan). All other chemicals were of the highest grade available and used without further purification.

ODNs. All ODNs used were purchased from Integrated DNA Technologies, Inc. (Coralville, IA, USA). The sequences of the ODNs are listed in Table S1. Each ODN was named, such as tripodna$_{36}$-1, with the base length as the subscript followed by the ODN number (#1 to #3 for tripodna, #1 to #4 for tetrapodna, and so on). For the cellular uptake experiments, fluorescently labeled tri-, tetra-, penta-, hexa-, and octapodna were prepared using Alexa Fluor 488-labeled tripodna$_{36}$-2 at the 5′ end, a common component of these polypodna preparations.

Preparation of Polypodna. Each polypodna was prepared by mixing equimolar amounts of ODNs as previously described.[22]

High-Speed AFM Imaging of Polypodna Preparations. AFM images were obtained on a high-speed AFM system (Nano Live Vision, RIBM, Tsukuba, Japan) using a silicon nitride cantilever (Olympus BL-AC10EGS).[44] In brief, the sample (2 μL) was adsorbed on a freshly cleaved mica plate pretreated with 0.1% aqueous 3-aminopropyltriethoxysilane for 5 min at room temperature and then washed three times with a buffer solution containing 20 mM Tris and 10 mM $MgCl_2$. Scanning was performed in the same buffer solution.

Measurement of Melting Temperature. The melting temperature (T_m) was obtained by measuring the absorbance of polypodna or other DNA preparations in a Tris HCl (TE) buffer solution (10 mM Tris, 1 mM EDTA, pH 8) containing 5 mM sodium chloride at 260 nm with a Shimadzu UV-1600 PC spectrometer (Kyoto, Japan) equipped with a TMSPC-8 temperature controller.[18] To estimate the thermal stability of polypodna in and outside of cells, the T_m of polypodna was also measured in TE buffer solutions of pH 7.4 (a simulated extracellular fluid containing 142 mM sodium, 4 mM potassium, and 5 mM calcium ions) and pH 5.5 (a simulated endosomal fluid containing 70 mM sodium and 32.5 mM potassium ions). These conditions of pH and ion concentrations were determined according to published data.[40]

Dynamic Light Scattering Analysis. The apparent size of polypodna was determined by the dynamic light scattering method using a Malvern Zetasizer 3000HS (Malvern Instruments, Malvern, UK) at 20 °C. The measurement was repeated at least three times, and the results were expressed as the mean because the standard error (SE) values were less than 5% of the mean in all cases.

CD Spectra of Polypodna and Other DNAs. The CD spectra of DNA were recorded using a JASCO-820 type spectropolarimeter (JASCO, Tokyo, Japan) at 4 °C with a 0.1 cm path-length quartz cell at 25 °C. The DNA samples after annealing were diluted with TE buffer containing 5 mM sodium chloride to a final DNA concentration of 25 μg/mL. The CD spectra of DNA were measured in the range of 200 to 320 nm.

Cell Cultures. Murine macrophage-like cells, RAW 264.7, were grown in RPMI1640 medium supplemented with 10% heat-inactivated FBS, 0.15% sodium bicarbonate, 100 units/mL penicillin, 100 mg/mL streptomycin, and 2 mM L-glutamine at 37 °C in humidified air containing 5% CO_2. Cells were then seeded on 24-well or 96-well culture plates at a density of 5×10^5 cells/mL and cultured for 24 h prior to use.

Cytokine Release from RAW264.7 Cells. RAW264.7 cells were seeded into 24-well plates at a density of 2.5×10^5 cells/well and incubated for 24 h before treatment. Then, ssDNA, dsDNA, or several type of polypodna diluted in 0.5 mL of Opti-MEM were added to cells. The cells were incubated for 8 h, and the supernatants were collected and stored at −70 °C until use. The levels of TNF-α and IL-6 in the supernatants were determined by enzyme-linked immunosorbent assay (ELISA) using OptEIATM sets (Pharmingen, San Diego, CA, USA).

Uptake of DNA in RAW264.7 Cells. RAW264.7 cells on 96-well plates at a density of 5×10^4 cells/well were incubated with Alexa Fluor 488-labeled ssDNA, dsDNA, or polypodna diluted in 0.1 mL of Opti-MEM for 8 h at 37 or 4 °C. Cells were then washed twice with 200 μL phosphate-buffered saline (PBS) and harvested. Then, the fluorescent intensity of cells was determined by flow cytometry (FACS Calibur, BD Biosciences, NJ, USA) using CellQuest software (version 3.1, BD Biosciences), and the mean fluorescence intensity (MFI) was calculated. Because the amount of Alexa Fluor 488-labeled ODN (tripodna$_{36}$-2) in the DNA samples was not identical, a normalized MFI was calculated as an indicator of cellular uptake of DNA preparations by multiplying the MFI obtained with the fraction of Alexa Fluor 488-labeled ODN in samples (*i.e.*, 3 for tripodna and 6 for hexapodna). In different sets of experiments, Alexa Fluor 488-labeled tripodna$_{36}$ or hexapodna$_{36}$ in Opti-MEM was added to RAW264.7 cells at a final concentration of 2 μg/mL with or without unlabeled DNA samples at a concentration of 2, 6, or 20 μg/mL. After 2 h incubation at 37 °C, the cells were treated as described above and the MFI was calculated. The uptake of polypodna consisting of 240 nucleotides was examined by measuring the disappearance of polypodna from culture media. Each polypodna diluted in 0.1 mL of Opti-MEM was added to RAW264.7 cells at a final concentration of 2 μg/mL. After 0, 1, 2, 4, 8, and 12 h of incubation, a 10 μL aliquot of culture media was transferred to plastic tubes and mixed with 20 μL of 0.5 M EDTA solution to stop the degradation and then stored at −20 °C until use. These samples were run on a 6% PAGE and stained with SYBR Gold (Molecular Probes, Eugene, OR, USA). The density of DNA bands was quantitatively evaluated using the Image Quant TL software (GE Healthcare Japan, Tokyo, Japan).

Fluorescence Microscopic Observation. RAW264.7 cells were seeded on 13 mm diameter glass coverslips and incubated for 24 h. The culture medium was replaced with Opti-MEM including Alexa Fluor 488-labeled hexapodna$_{36}$. After incubation at 37 °C for 3 h, cells were washed three times with PBS, fixed with 4% paraformaldehyde for 20 min, and washed again three times with PBS. Then, 60 nM 4′,6-diamino-2-phenylindole (DAPI) was added to stain the nuclei and washed three times with PBS after 10 min incubation. Then, the coverslips were mounted on glass slides with SlowFade Gold (Invitrogen, Carlsbad, CA, USA) and observed using a fluorescence microscope (Biozero BZ-8000, KEYENCE, Osaka, Japan).

Stability of Polypodna in Serum. Polypodna preparations were incubated with 20% mouse serum diluted with RPMI1640 medium at a concentration of 10 μg/100 μL at 37 °C. After 0, 2, 4, 8, 12, or 24 h of incubation, a 10 μL aliquot of the sample solution was transferred to plastic tubes and mixed with 20 μL of 0.5 M EDTA solution to stop the degradation and then stored at −20 °C until use. These samples were run on a 12% PAGE at 4 °C and stained with SYBR Gold (Molecular Probes). The density of DNA bands was quantitatively evaluated using the Multi Gauge software (FUJIFILM, Tokyo, Japan).

Statistical Analysis. Differences were statistically evaluated by one-way analysis of variance (ANOVA) followed by the Fisher's PLSD test for multiple comparisons. A P value of <0.05 was considered to be statistically significant.

Conflict of Interest: The authors declare no competing financial interest.

Acknowledgment. This work was supported in part by a Grant-in-Aid for Scientific Research (B) (23390010).

Supporting Information Available: Oligonucleotide sequences used in this study, disappearance of polypodna preparations consisting of 240 nucleotides from culture media of RAW264.7

cells, and uptake of Alexa Fluor 488-labeled hexapodna$_{36}$ in RAW264.7 cells. This material is available free of charge *via* the Internet at http://pubs.acs.org.

REFERENCES AND NOTES

1. Lee, J. B.; Roh, Y. H.; Um, S. H.; Funabashi, H.; Cheng, W.; Cha, J. J.; Kiatwuthinon, P.; Muller, D. A.; Luo, D. Multifunctional Nanoarchitectures from DNA-Based ABC Monomers. *Nat. Nanotechnol.* **2009**, *4*, 430–436.
2. Takada, T.; Fujitsuka, M.; Majima, T. Single-Molecule Observation of DNA Charge Transfer. *Proc. Natl. Acad. Sci. U.S.A.* **2007**, *104*, 11179–11183.
3. Nishikawa, M.; Rattanakiat, S.; Takakura, Y. DNA-Based Nano-Sized Systems for Pharmaceutical and Biomedical Applications. *Adv. Drug Delivery Rev.* **2010**, *62*, 626–632.
4. Kawai, T.; Akira, S. The Role of Pattern-Recognition Receptors in Innate Immunity: Update on Toll-like Receptors. *Nat. Immunol.* **2010**, *11*, 373–384.
5. Krieg, A. M. CpG Motifs in Bacterial DNA and Their Immune Effects. *Annu. Rev. Immunol.* **2002**, *20*, 709–760.
6. Vollmer, J.; Krieg, A. M. Immunotherapeutic Applications of CpG Oligodeoxynucleotide TLR9 Agonists. *Adv. Drug Delivery Rev.* **2009**, *61*, 195–204.
7. Gupta, G. K.; Agrawal, D. K. CpG Oligodeoxynucleotides as TLR9 Agonists: Therapeutic Application in Allergy and Asthma. *BioDrugs* **2010**, *24*, 225–235.
8. Klinman, D. M. Immunotherapeutic Uses of CpG Oligodeoxynucleotides. *Nat. Rev. Immunol.* **2004**, *4*, 249–258.
9. Krieg, A. M. Therapeutic Potential of Toll-like Receptor 9 Activation. *Nat. Rev. Drug Discovery* **2006**, *5*, 471–484.
10. Grünweller, A.; Wyszko, E.; Bieber, B.; Jahnel, R.; Erdmann, V. A.; Kurreck, J. Comparison of Different Antisense Strategies in Mammalian Cells Using Locked Nucleic Acids, 2′-O-Methyl RNA, Phosphorothioates and Small Interfering RNA. *Nucleic Acids Res.* **2003**, *31*, 3185–3193.
11. Sheehan, J. P.; Lan, H. C. Phosphorothioate Oligonucleotides Inhibit the Intrinsic Tenase Complex. *Blood* **1998**, *92*, 1617–1625.
12. Brown, D. A.; Kang, S. H.; Gryaznov, S. M.; DeDionisio, L.; Heidenreich, O.; Sullivan, S.; Xu, X.; Nerenberg, M. I. Effect of Phosphorothioate Modification of Oligodeoxynucleotides on Specific Protein Binding. *J. Biol. Chem.* **1994**, *269*, 26801–26805.
13. Levin, A. A. A Review of the Issues in the Pharmacokinetics and Toxicology of Phosphorothioate Antisense Oligonucleotides. *Biochim. Biophys. Acta* **1999**, *1489*, 69–84.
14. Henry, S. P.; Beattie, G.; Yeh, G.; Chappel, A.; Giclas, P.; Mortari, A.; Jagels, M. A.; Kornbrust, D. J.; Levin, A. A. Complement Activation Is Responsible for Acute Toxicities in Rhesus Monkeys Treated with a Phosphorothioate Oligodeoxynucleotide. *Int. Immunopharmacol.* **2002**, *2*, 1657–1666.
15. Schmidt, M.; Anton, K.; Nordhaus, C.; Junghans, C.; Wittig, B.; Worm, M. Cytokine and Ig-Production by CG-Containing Sequences with Phosphorodiester Backbone and Dumbbell-Shape. *Allergy* **2006**, *61*, 56–63.
16. Li, J.; Pei, H.; Zhu, B.; Liang, L.; Wei, M.; He, Y.; Chen, N.; Li, D.; Huang, Q.; Fan, C. Self-Assembled Multivalent DNA Nanostructures for Noninvasive Intracellular Delivery of Immunostimulatory CpG Oligonucleotides. *ACS Nano* **2011**, *5*, 8783–8789.
17. Nishikawa, M.; Matono, M.; Rattanakiat, S.; Matsuoka, N.; Takakura, Y. Enhanced Immunostimulatory Activity of Oligodeoxynucleotides by Y-Shape Formation. *Immunology* **2008**, *124*, 247–255.
18. Matsuoka, N.; Nishikawa, M.; Mohri, K.; Rattanakiat, S.; Takakura, Y. Structural and Immunostimulatory Properties of Y-Shaped DNA Consisting of Phosphodiester and Phosphorothioate Oligodeoxynucleotides. *J. Controlled Release* **2010**, *148*, 311–316.
19. Li, Y.; Tseng, Y. D.; Kwon, S. Y.; D'Espaux, L.; Bunch, J. S.; McEuen, P. L.; Luo, D. Controlled Assembly of Dendrimer-like DNA. *Nat. Mater.* **2004**, *3*, 38–42.
20. Um, S. H.; Lee, J. B.; Park, N.; Kwon, S. Y.; Umbach, C. C.; Luo, D. Enzyme-Catalysed Assembly of DNA Hydrogel. *Nat. Mater.* **2006**, *5*, 797–801.
21. Rattanakiat, S.; Nishikawa, M.; Funabashi, H.; Luo, D.; Takakura, Y. The Assembly of a Short Linear Natural Cytosine-Phosphate-Guanine DNA into Dendritic Structures and Its Effect on Immunostimulatory Activity. *Biomaterials* **2009**, *30*, 5701–5706.
22. Nishikawa, M.; Mizuno, Y.; Mohri, K.; Matsuoka, N.; Rattanakiat, S.; Takahashi, Y.; Funabashi, H.; Luo, D.; Takakura, Y. Biodegradable CpG DNA Hydrogels for Sustained Delivery of Doxorubicin and Immunostimulatory Signals in Tumor-Bearing Mice. *Biomaterials* **2011**, *32*, 488–494.
23. Rothemund, P. W. Folding DNA To Create Nanoscale Shapes and Patterns. *Nature* **2006**, *440*, 297–302.
24. He, Y.; Ye, T.; Su, M.; Zhang, C.; Ribbe, A. E.; Jiang, W.; Mao, C. Hierarchical Self-Assembly of DNA into Symmetric Supramolecular Polyhedra. *Nature* **2008**, *452*, 198–201.
25. Seeman, N. C. Nanomaterials Based on DNA. *Annu. Rev. Biochem.* **2010**, *79*, 65–87.
26. Lee, J. B.; Campolongo, M. J.; Kahn, J. S.; Roh, Y. H.; Hartman, M. R.; Luo, D. DNA-Based Nanostructures for Molecular Sensing. *Nanoscale* **2010**, *2*, 188–197.
27. Yang, D.; Campolongo, M. J.; Nhi Tran, T. N.; Ruiz, R. C.; Kahn, J. S.; Luo, D. Novel DNA Materials and Their Applications. *Wiley Interdiscip. Rev. Nanomed. Nanobiotechnol.* **2010**, *2*, 648–669.
28. Mizuno, R.; Haruta, H.; Morii, T.; Okada, T.; Asakawa, T.; Hayashi, K. Synthesis and AFM Visualization of DNA Nanostructures. *Thin Solid Films* **2004**, *464–465*, 459–463.
29. Lyubchenko, Y. L.; Shlyakhtenko, L. S.; Ando, T. Imaging of Nucleic Acids with Atomic Force Microscopy. *Methods* **2011**, *54*, 274–283.
30. Wang, X.; Seeman, N. C. Assembly and Characterization of 8-arm and 12-arm DNA Branched Junctions. *J. Am. Chem. Soc.* **2007**, *129*, 8169–8176.
31. Altona, C.; Pikkemaat, J. A.; Overmars, F. J. Three-Way and Four-Way Junctions in DNA: A Conformational Viewpoint. *Curr. Opin. Struct. Biol.* **1996**, *6*, 305–316.
32. Kypr, J.; Kejnovská, I.; Renciuk, D.; Vorlícková, M. Circular Dichroism and Conformational Polymorphism of DNA. *Nucleic Acids Res.* **2009**, *37*, 1713–1725.
33. Tozuka, Y.; Yoshikawa, Y.; Ohishi, H.; Kobayashi, Y.; Da-Yang, Z.; Nakatani, K. Measurement of Circular Dichroism and Structural Chemical Research of d(CG)$_6$ and d(TA)$_6$. *Nucleic Acids Symp. Ser.* **2006**, *50*, 227–228.
34. Roberts, T. L.; Dunn, J. A.; Terry, T. D.; Jennings, M. P.; Hume, D. A.; Sweet, M. J.; Stacey, K. J. Differences in Macrophage Activation by Bacterial DNA and CpG-Containing Oligonucleotides. *J. Immunol.* **2005**, *175*, 3569–3576.
35. Kumagai, Y.; Takeuchi, O.; Akira, S. TLR9 as a Key Receptor for the Recognition of DNA. *Adv. Drug Delivery Rev.* **2008**, *60*, 795–804.
36. Takeshita, F.; Gursel, I.; Ishii, K. J.; Suzuki, K.; Gursel, M.; Klinman, D. M. Signal Transduction Pathways Mediated by the Interaction of CpG DNA with Toll-like Receptor 9. *Semin. Immunol.* **2004**, *16*, 17–22.
37. Ciafrè, S. A.; Rinaldi, M.; Gasparini, P.; Seripa, D.; Bisceglia, L.; Zelante, L.; Farace, M. G.; Fazio, V. M. Stability and Functional Effectiveness of Phosphorothioate Modified Duplex DNA and Synthetic 'Mini-genes". *Nucleic Acids Res.* **1995**, *23*, 4134–4142.
38. Rutz, M.; Metzger, J.; Gellert, T.; Luppa, P.; Lipford, G. B.; Wagner, H.; Bauer, S. Toll-like Receptor 9 Binds Single-Stranded CpG-DNA in a Sequence- and pH-Dependent Manner. *Eur. J. Immunol.* **2004**, *34*, 2541–2550.
39. Latz, E.; Verma, A.; Visintin, A.; Gong, M.; Sirois, C. M.; Klein, D. C.; Monks, B. G.; McKnight, C. J.; Lamphier, M. S.; Duprex, W. P.; *et al.* Ligand-Induced Conformational Changes Allosterically Activate Toll-like Receptor 9. *Nat. Immunol.* **2007**, *8*, 772–779.
40. Scott, C. C.; Gruenberg, J. Ion Flux and the Function of Endosomes and Lysosomes: pH Is Just the Start: The Flux of Ions across Endosomal Membranes Influences Endosome Function Not Only through Regulation of the Luminal pH. *Bioessays* **2011**, *33*, 103–110.
41. Hamzah, J.; Altin, J. G.; Herringson, T.; Parish, C. R.; Hämmerling, G. J.; O'Donoghue, H.; Ganss, R. Targeted

Liposomal Delivery of TLR9 Ligands Activates Spontaneous Antitumor Immunity in an Autochthonous Cancer Model. *J. Immunol.* **2009**, *183*, 1091–1098.
42. Wei, M.; Chen, N.; Li, J.; Yin, M.; Liang, L.; He, Y.; Song, H.; Fan, C.; Huang, Q. Polyvalent Immunostimulatory Nanoagents with Self-Assembled CpG Oligonucleotide-Conjugated Gold Nanoparticles. *Angew. Chem., Int. Ed.* **2012**, *51*, 1202–1206.
43. Schüller, V. J.; Heidegger, S.; Sandholzer, N.; Nickels, P. C.; Suhartha, N. A.; Endres, S.; Bourquin, C.; Liedl, T. Cellular Immunostimulation by CpG-Sequence-Coated DNA Origami Structures. *ACS Nano* **2011**, *5*, 9696–9702.
44. Endo, M.; Katsuda, Y.; Hidaka, K.; Sugiyama, H. Regulation of DNA Methylation Using Different Tensions of Double Strands Constructed in a Defined DNA Nanostructure. *J. Am. Chem. Soc.* **2010**, *132*, 1592–1597.